Impact on Granular Beds

Devaraj van der Meer

Physics of Fluids Group, MESA+ Institute for Nanotechnology, and Faculty of Science and Technology, University of Twente, 7500AE Enschede, The Netherlands;
email: d.vandermeer@utwente.nl

Annu. Rev. Fluid Mech. 2017. 49:463–84

First published online as a Review in Advance on August 25, 2016

The *Annual Review of Fluid Mechanics* is online at fluid.annualreviews.org

This article's doi:
10.1146/annurev-fluid-010816-060213

Keywords

crater, drag, impact, granular flow, granular solid, interstitial fluid, jet, splash

Abstract

The impact of an object on a granular solid is an ubiquitous phenomenon in nature, the scale of which ranges from the impact of a raindrop onto sand all the way to that of a large asteroid on a planet. Despite the obvious relevance of these impact events, the study of the underlying physics mechanisms that guide them is relatively young, with most work concentrated in the past decade. Upon impact, an object starts to interact with a granular bed and experiences a drag force from the sand. This ultimately leads to phenomena such as crater formation and the creation of a transient cavity that upon collapse may cause a jet to appear from above the surface of the sand. This review provides an overview of research that targets these phenomena, from the perspective of the analogous but markedly different impact of an object on a liquid. It successively addresses the drag an object experiences inside a granular bed, the expansion and collapse of the cavity created by the object leading to the formation of a jet, and the remarkable role played by the air that resides within the pores between the grains.

1. INTRODUCTION: IMPACT CRATERS, JETS, SPLASHES, AND ERUPTIONS

A classical free-surface-flow experiment is one in which an object is dropped onto a quiescent liquid pool and creates a splash. Ever since the advent of photography and the pioneering work of Worthington, who produced a book full of beautiful pictures containing a wealth of physics insight (Worthington 1908), these types of phenomena have intrigued scientists and continue to do so today. In the past few decades, the development of high-speed photography (Thoroddsen et al. 2008, Versluis 2013) and availability of adequate numerical techniques to simulate free-surface flows, such as the boundary integral technique and level-set methods, have boosted research in this area, leading to a tremendous increase of our knowledge in this steeply developing field.

The question addressed in this review is, what happens when the liquid substrate is replaced by a bed of grains; that is, what happens when a projectile lands in a sandy desert instead of onto the sea? Such situations are ubiquitous in nature, where one needs only think of the impact of a meteorite on the moon or a raindrop falling onto soil. But these types of impacts are also relevant to agriculture and industry, e.g., in wet granulation, the basis of the production of many pharmaceuticals.

Granular materials, depending on the circumstances, may behave like a solid, liquid, or gas (Jaeger et al. 1996a,b; de Gennes 1999; Kadanoff 1999; Aranson & Tsimring 2006). Before impacts, such a granular substrate is typically in a solid-like state and fluidizes only as a result of the impact. In contrast to what happens during impact on a liquid, the impactor needs to overcome a threshold yield stress to penetrate into a granular bed, where the magnitude of this yield stress depends on the way the material is packed. Moreover, granular materials effectively dissipate the energy being imparted on them, and do so in ways that are partly distinct from viscous dissipation in an ordinary liquid. Nevertheless, with the pioneering work of Thoroddsen & Shen (2001), it became clear that during and after impact on sand, phenomena may be observed that are remarkably similar to those in a liquid.

Figure 1 compares the impact of a steel sphere on a bed of very loosely packed, fine sand to that of a disk onto water. From left to right, one sees the object before impact, the splash created upon impact, and the jet that subsequently shoots up from the substrate. Clearly, the visible events are similar for both cases. However, in the liquid, one can actually observe what happens within the substrate: Upon impact, an expanding cavity is created in the wake of the impactor, which subsequently collapses because of the hydrostatic pressure in the liquid and pinches off in a single point at the axis of symmetry. From this pinch-off point, two jets are created: one shooting upward and the other one downward.

Often, when a jet is formed during impact, the process concludes with the emergence of a granular eruption at the end of the impact sequence. This eruption is associated with the surfacing of an air bubble that is entrapped during the pinch-off process and subsequently slowly rises through the granular bed after the emergence of the jet. Finally, an impact crater is often formed as a remnant of the event long after the impact has taken place (Ruiz Suárez 2013). This is comparable to the large-scale asteroid impacts that have left their visible marks all over our solar system, for example, craters on the moon or Mars. These craters are even observable on Earth, either very prominently (e.g., the famous Barringer crater in Arizona, with a diameter of 1.3 km) or concealed (e.g., the enormous Chicxulub crater, the remnants of which spread over a large part of the Yucatán peninsula in Mexico) (Melosh 1989, Holsapple 1993, Melosh & Ivanov 1999, Holsapple et al. 2002, Pierazzo & Collins 2004).

This brings us to the formulation of the main purpose of this review, which is to discuss research efforts during the past two decades that have strived to answer the following questions: What laws

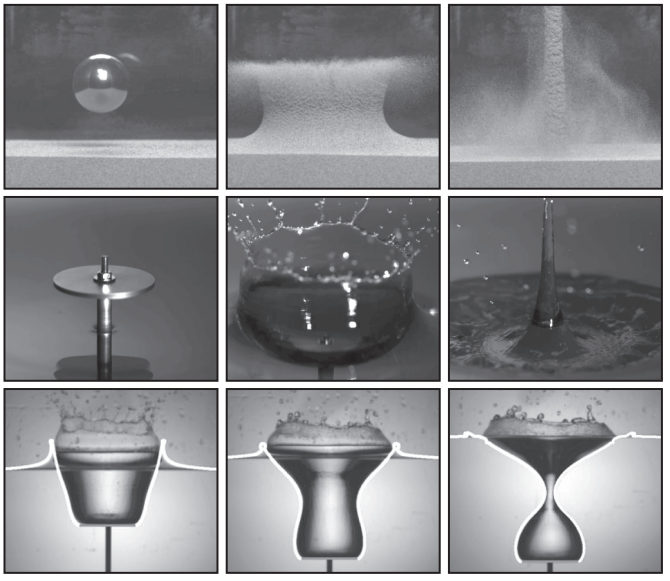

Figure 1

(*Top row*) Impact of a steel sphere on a bed of very loosely packed, fine sand compared to (*middle row*) that of a disk onto water. Time increases from left to right, and one subsequently observes the object just before impact, the splash, and the jet that shoots up from the substrate. (*Bottom row*) Cavity formation and collapse in a liquid. Figure adapted with permission from Lohse et al. (2004a) (*top row*) and Bergmann et al. (2009) (*bottom row*). Copyright 2004 by the American Physical Society and 2009 by Cambridge University Press.

govern the penetration of an object into a granular bed, and what is the role of the packing fraction? To what extent is the granular jet created by a mechanism similar to that of a liquid impact jet? What is the role of interstitial air in the process of jet formation? Finally, what happens when the impacting object is replaced by a deformable liquid drop? The organization of this review is precisely along the questions formulated above, with a section dedicated to each of them.

In recent years, many fine books and review articles have appeared on the subject of granular materials. There are, however, two works that deserve special mention because their topics are close to that of the current review. First, in an excellent review, Ruiz Suárez (2013) discusses the penetration of projectiles into granular targets, largely focusing on crater formation, thus being complementary to the current review, which focuses on drag, jet formation, and the role of interstitial fluid. Second, the recent monograph *Physics of Soft Impact and Cratering* (Katsuragi 2016) serves as an excellent textbook for readers interested in the concepts and physics that lie behind the works discussed in the current review.

2. IMPACTOR DYNAMICS: DRAG ON AN OBJECT IN SAND

When an object moves through a liquid, it experiences a drag force that is either proportional to the velocity of the object (Stokes' drag) when viscous forces dominate or proportional to the velocity squared (quadratic or inertial drag) in the regime where inertial forces are dominant. This is textbook knowledge, but less well known is that when an object impacts onto a liquid, there may be a third important contribution that occurs when a cavity is opening behind the object. When a downward-moving object is fully immersed in a liquid, the (hydrostatic) pressure integral over the leading (or front) edge of the body is almost compensated by that over the trailing (or rear)

edge, with the difference constituting the objects' buoyancy force. However, in the presence of a cavity in the wake of the object that is open toward the top, the trailing-edge integral reduces to an integral over the atmospheric pressure. In this case, the leading-edge integral gives rise to an additional drag term, which is proportional to the hydrostatic pressure inside the liquid, and therefore to the depth of the object below the liquid surface.

In a granular material, certain aspects are similar, whereas others are different: When the object penetrates downward into the granular bed, it experiences an upward drag force, just like in a liquid, and many studies have been devoted to how this drag force depends on the impact parameters, which is discussed in some detail below. There is, however, one very different feature, namely that the object usually comes to a full stop within the bulk of the granular bed. Because gravity is still acting on the penetrating object, this implies that the drag force has thus been substituted by an opposing static force that keeps the object in its position. Many authors have acknowledged this and have also noted that usually there is a discontinuity in the drag force (or acceleration) just before the object comes to a full stop, indicating that this static force is of a different nature than the (dynamic) drag force (Katsuragi & Durian 2007, Goldman & Umbanhowar 2008, Umbanhowar & Goldman 2010). This is reminiscent of an object sliding down an inclined plane, where the dynamic friction experienced while sliding is usually different from the static friction that balances the in-plane component of gravity when it has come to a standstill.

2.1. Drag: Position Measurements

In agreement with mentioned observations from the liquid literature, scientists have proposed various expressions for the drag force a body experiences when it penetrates into a granular solid. Perhaps the oldest account of such a model is that of Poncelet (1829), which assumes that the drag force acting on the object consists of a constant resistance force and a quadratic drag term (Allen et al. 1957, Backman & Goldsmith 1978). While studying the formation of impact craters (Walsh et al. 2003), de Bruyn & Walsh (2004) described their granular bed as a Bingham (or yield-stress) material, which in their case led to a drag force with a constant resistance force and a Stokes' drag term. The viscosity in the latter was motivated by their experiments on dimensional grounds. An obvious problem with such a model is that if gravity exceeds the drag force, the object continues to move down at a constant speed, the so-called terminal velocity, which contradicts experimental observations.

In the same year, Lohse et al. (2004b) studied the motion of a sphere released with negligible velocity onto a bed of very loose, fine sand (Lohse et al. 2004a) and noted that their results could be described with a drag force that increased linearly with the depth z of the object's location under the surface of the sand bed, i.e., a force that is proportional to the hydrostatic (or lithostatic) pressure at depth z, caused by the weight of the granular material above that point. They argued that, for the object to move deeper, work needs to be performed against this hydrostatic pressure, by displacing granular material and by Coulomb friction between the ball and sand grains.

A large step forward was taken by the Durian group, who investigated several aspects of impact on loose granular beds (Newhall & Durian 2003; Uehara et al. 2003; Ambroso et al. 2005a,b; Nelson et al. 2008). Katsuragi & Durian (2007) showed that the drag force in a large number of experiments was described by a unified force law for the drag (proposed earlier in Boguslavskii et al. 1996a,b; Volfson et al. 2003; Tsimring & Volfson 2005; Hinch 2014):

$$F_{\mathrm{drag}} = -kz - \alpha v^2, \tag{1}$$

where v is the velocity of the object, z is its depth below the (quiescent) surface of the bed, and k and α are constants. That is, the drag law for loose granular beds was found to consist of a hydrostatic

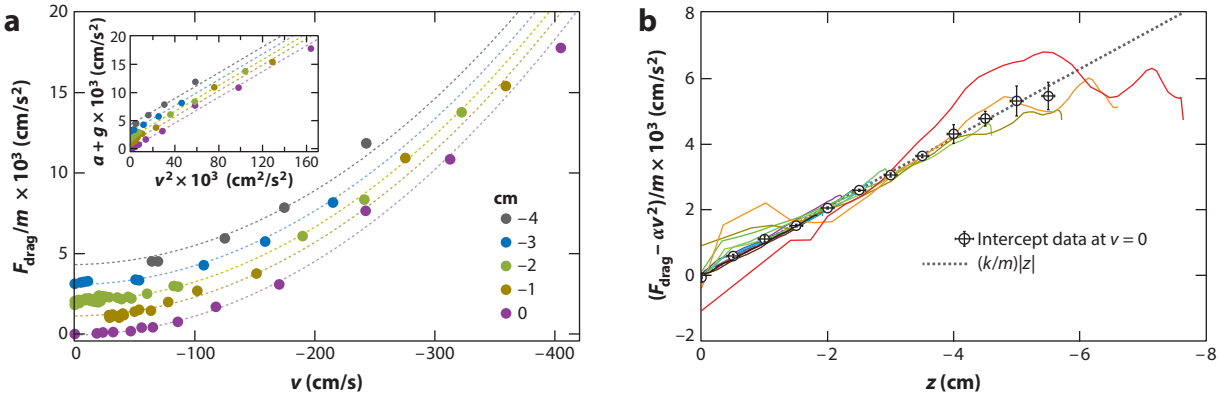

Figure 2

Experimental evidence for the universal drag force law. (*a*) For a fixed depth z, the acceleration due to drag F_{drag}/m scales as velocity v squared. (*b*) Once the velocity-dependent term $\alpha v^2/m$ is subtracted from F_{drag}/m, the result is proportional to the depth z. The colored solid curves correspond to different impact velocities between 0 and 4.0 m/s. Figure adapted from Katsuragi & Durian (2007) with permission from Macmillan Publishers Ltd.: Nature Physics, copyright 2007.

drag term and a quadratic drag term (see **Figure 2** and the sidebar The Hydrostatic Drag Term). The validity of Equation 1 for loose beds was confirmed by others (Ciamarra et al. 2004; Hou et al. 2005a,b; Royer et al. 2008; von Kann et al. 2010; Royer et al. 2011), but departures from it were observed as soon as finite container size effects started to play a role. Katsuragi & Durian (2013) related the coefficients in Equation 1 to the impact parameters. Whereas the quadratic term was found to scale as can be deduced on dimensional grounds ($\alpha \sim A\rho_g$, with ρ_g the density of the granular medium and A the cross-sectional area of the impactor), this turned out not to be the case for the hydrostatic term for which $k \sim A\rho_g$ was expected, but a nontrivial and hitherto unexplained dependence on the impactor density ρ_i was found, namely $k \sim A(\rho_g\rho_i)^{1/2}$.

2.2. Drag: Direct Acceleration Measurements

All of the previously mentioned experiments were performed using a visual measurement of the position of the object inside the granular bed, mostly by attaching a rod to the object such that it becomes observable above the bed, but sometimes using more sophisticated techniques like X-ray imaging (e.g., Royer et al. 2011). Because accelerations and forces are obtained by numerically taking the second derivative from the data, it may be expected that some details remain concealed.

THE HYDROSTATIC DRAG TERM

In impact onto a liquid, a hydrostatic drag term of the form $F_{drag} = -kz$ is only expected when a cavity is created above the impacting object that is open toward the surroundings. However, such a term always exists within a granular bed. This is because several phenomena break the symmetry between the pressure on the lower (leading-edge) side of the object and that on the top (trailing-edge) side, also in the absence of such a cavity. One is the effect of arching, in which forces on the trailing edge are shielded by arch-like structures that the grains may be forming above the downward-moving object. Another one is that grains are locally pressed together on the leading edge, which may lead to larger frictional forces on the front as compared to the back.

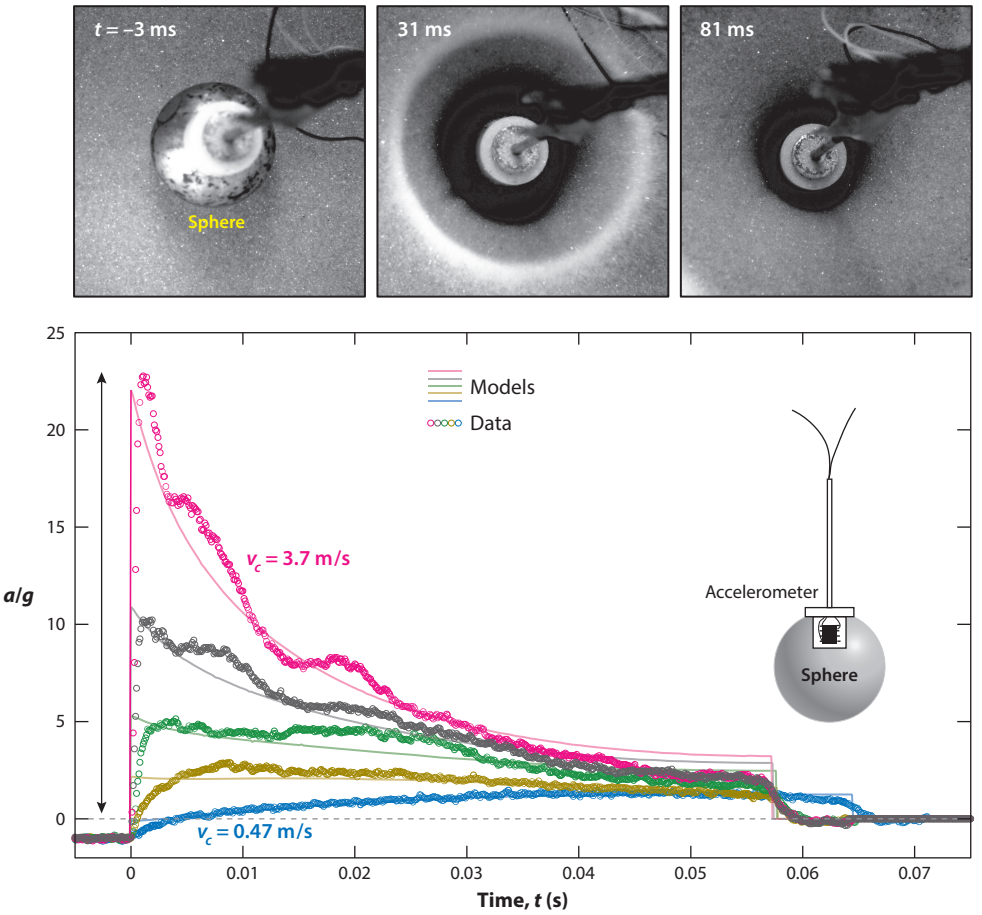

Figure 3

Direct measurement of the drag force inside a granular bed using an accelerometer: (*top panels*) snapshots of the experiment and (*bottom panel*) the time evolution of the measured acceleration. The model of Equation 1 (*solid lines*) reasonably fits the data (*circles*), but there are clear differences that increase with velocity. Figure adapted with permission from Goldman & Umbanhowar (2008). Copyright 2008 by the American Physical Society.

More recently, position-based measurements have been complemented by direct measurements of the force that the impactor experiences. The first extensive study (Goldman & Umbanhowar 2008) used a wired accelerometer glued to the impactor (**Figure 3**); although results were largely in agreement with the force law of Equation 1, additional structures were revealed that went unnoticed from the position data. **Figure 3** provides an example of the acceleration data. The model of Equation 1 more or less follows the experimental data, but there are also discrepancies, such as the behavior observed for larger velocities in which the data appear to oscillate around the theoretical curve. A satisfactory explanation for these observations is still lacking.

Joubaud et al. (2014), and simultaneously Altshuler et al. (2014), noninvasively measured the acceleration using an instrumented particle containing an accelerometer that sends its data radiographically to an external controller. For impact onto a very loose bed of fine sand, they observed

a clear influence of the closure of the cavity and the production of the jet: Whereas the drag acceleration data first follow the theory reasonably well, a sharp spike is observed at the moment the cavity closes and the jet is produced. This event continues to influence the measured acceleration of the downward-moving particle for the rest of the trajectory, during which it is found to not be accurately described by the drag law of Equation 1.

In a second paper, Umbanhowar & Goldman (2010) included the systematic study of an important parameter into the problem, namely the packing fraction φ of the granular bed. Whereas most of the data discussed so far had been obtained in (very) loose beds, Umbanhowar & Goldman (2010) carefully controlled the packing of the bed and found that Equation 1 performed best for what they called the critical packing state, which is the packing fraction for which no dilation or compression of the granular material occurs under shear (Schofield & Wroth 1968, Schröter et al. 2007). Below and above this critical φ, the prefactor of the quadratic term in Equation 1 depends on depth and, for the hydrostatic term, a Jansen-type response (Janssen 1895, Sperl 2006) is found, in which a saturation of the hydrostatic pressure occurs for larger depths.

Packing fraction: ratio of the volume occupied by the solid phase (grains) and the total volume of the granular medium

Dilation: effect that the volume of a dense granular medium needs to expand to allow for motion

2.3. Micromechanics and Numerical Simulations

In addition to the above-mentioned work that studies the continuum approach to the drag force an object experiences inside a granular bed, there are several excellent papers that concentrate on the micromechanical aspects of the drag, e.g., by measuring the forces between individual grains and the resulting force-chain networks during impact. On the one hand, this is done experimentally, using the technique developed by the Behringer group in which the stress in photoelastic discs is measured and converted into contact forces (Daniels et al. 2004; Clark et al. 2012, 2014; Clark & Behringer 2013) or using 3D imaging techniques (Nordstrom et al. 2014). In an example of the first technique, **Figure 4*a*** presents an image from the impact of a large disk onto a 2D granular medium consisting of photoelastic disks. On its way to the camera, the light passes through cross polarizers, such that the more stress a disk experiences, the brighter it shows up in the image.

On the other hand, there is significant use of numerical techniques to obtain quantities characterizing the interactions on the particle scale during impact. Some of these describe the particle-particle and particle-intruder interactions using hard-sphere or soft-sphere spring-dashpot

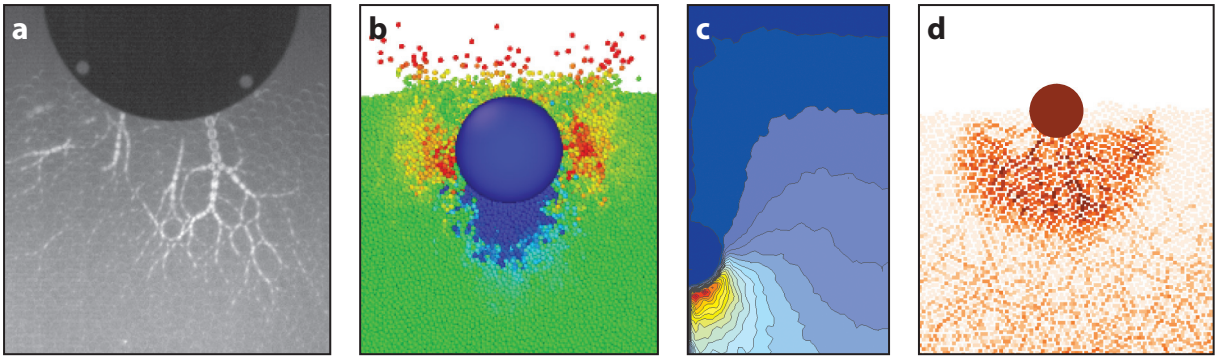

Figure 4

(*a*) Image from the impact of a large disk onto a granular medium consisting of photoelastic disks, showing the force chains below the impactor. Panel *a* taken with permission from Clark et al. (2012). (*b*) Snapshot and (*c*) pressure field during the impact of a sphere on a bed of grains, simulated with a numerical code that includes air. Panels *b* and *c* taken with permission from Xu et al. (2014). (*d*) Numerical simulation of the impact of a disk, showing the normal forces experienced by 2D granular particles. Panel *d* taken with permission from Kondic et al. (2012). All panels copyright 2012 and 2014 by the American Physical Society.

contact models (Dwivedi et al. 2008, Ben-Dor et al. 2009, Seguin et al. 2009, Kondic et al. 2012) (**Figure 4*d***). There are also methods that additionally implement the airflow through the porous medium that is formed by the granular bed and are capable of—at least partly—capturing the air-mediated type of interactions that are present in loosely packed beds of fine grains (Xu et al. 2013, 2014). These numerical models were originally developed to describe the dynamics of gas-fluidized beds, which are ubiquitous in process technology. In them, typically, the airflow is modeled on a coarser grid, with each grid cell containing multiple particles, and empirical closure relations containing the local packing fraction and the average velocity differences between the two phases (e.g., the Ergun equation) are used to implement the forcing of the particle phase on the fluid phase (van der Hoef et al. 2008).

Added mass: the amount of a medium that needs to be accelerated together with an object when the object is accelerated

Typically, both the experimental and numerical micromechanical work have an intruder–to–particle size ratio that is much smaller than that used in most of the continuum approach experiments. In the latter, one typically deals with numbers of particles exceeding 10^{10}, a huge figure for which numerical simulation is still unfeasible. The ever increasing computer power and implementation of GPU techniques, however, should bring simulation and experiments closer together in the very near future. For example, it is not currently possible to directly compare the experiments discussed in Sections 3 and 4 with numerical simulations such as those discussed in Xu et al. (2014). However, such a comparison will be crucial for a better understanding of the role played by air in these systems.

2.4. Other Experiments: Added Mass and Superlight Materials

When an object moves through a liquid, there exists a so-called added mass, a volume of liquid that needs to be accelerated together with the object when the latter is accelerated. It stands to reason that in a granular bed there would also be such an added mass of grains that needs to be accelerated together with the penetrating object. Lohse et al. (2004b) included an added mass m_A in the equation of motion that was modeled based on the motion of a sphere through a liquid, which has an added mass corresponding to that of half its volume of liquid:

$$(m + m_A)\ddot{z} = mg + F_{drag}, \tag{2}$$

where m is the mass of the object itself and g the acceleration of gravity. Of course, this was done to obtain a more reliable expression because the size of the added mass in a bed of grains not only is unknown, but also likely depends on many parameters, most prominently the packing fraction φ of the bed. There is substantial evidence that such an added mass is there, and that it is appreciable. First, upon impact Goldman & Umbanhowar (2008) found an acceleration spike that corresponds to the loss of momentum an object experiences when it suddenly has to accelerate a certain amount of grains to its own velocity. Second, there are X-ray measurements in which a compacted region below the impacting object is observed (Royer et al. 2011, Homan et al. 2015), which is likely to contribute to the added mass. Finally, there is direct evidence of the added mass from force measurements in a recent paper on jumping on granular media (Aguilar & Goldman 2016).

Another line of research searches to be closer to the actual impact of asteroids on soil. Most noteworthy are papers from the Ruiz-Suárez group in which the solid object is replaced by a ball of consolidated grains (Pacheco-Vázquez & Ruiz-Suárez 2011, Bartali et al. 2013, González Gutiérrez et al. 2014) and the simultaneous impact of multiple objects is studied (as meteors often fragment before impact) (Pacheco-Vázquez & Ruiz-Suárez 2010, Solano-Altamirano et al. 2013). The same group also studied the drag on an object moving over large vertical distances through a superlight granular medium consisting of expanded polystyrene spheres, where drag obtains an even more fluid-like character (Pacheco-Vázquez & Ruiz-Suárez 2009, Pacheco-Vázquez et al. 2011).

3. GRANULAR BED DYNAMICS

This section focuses on the dynamics of a granular bed in the most pronounced case, namely when a jet is being produced. We start again from the analogy with a liquid in which, for a nonwetting (axisymmetric) object (Duclaux et al. 2007), an elongated cavity is being produced at the liquid surface when the impact velocity is sufficiently high. This elongated cavity subsequently collapses under the influence of the hydrostatic pressure in the liquid, and from the pinch-off point, two jets are formed: one going upward and one going downward. For an elongated cavity, this collapse can be described using potential flow (Gekle et al. 2009), and the cavity collapse can be modeled approximatively using a two-dimensional (2D) version of the Rayleigh-Bésant equation for the time evolution of the cavity radius $R(t)$:

$$(\ddot{R} + \dot{R}^2)\log(R/R_\infty) + \frac{1}{2}\dot{R}^2 = gz, \tag{3}$$

where R_∞ is a radius at which the flow field can be assumed to be decayed to zero (typically of the order of the cavity depth), and $\dot{R}$ and $\ddot{R}$ denote the first- and second-order time derivative of $R(t)$, respectively (Bergmann et al. 2006). In this picture, the cavity collapses in noninteracting horizontal layers (see the sidebar The 2D Rayleigh Equation and the Cavity Profile). For each depth z, Equation 3 is now solved, using the initial conditions for the radius R and the

THE 2D RAYLEIGH EQUATION AND THE CAVITY PROFILE

The 2D version of the Rayleigh-Bésant equation can easily be derived from the radial component of the 2D Euler equation for an ideal fluid:

$$\frac{\partial u_r}{\partial t} + u_r\frac{\partial u_r}{\partial r} = -\frac{1}{\rho}\frac{\partial p}{\partial r},$$

where u_r is the radial component of the velocity field (and we have assumed on symmetry grounds that the azimuthal component u_ϕ equals zero), r the radial coordinate, p the pressure field, and ρ the fluid density. The flow field u_r must be continuous up to the cavity wall; therefore, mass conservation implies that $u_r = R\dot{R}/r$. Inserting this expression into the first term of the above equation and integrating from $r = R_\infty$, where $u_r = 0$ and $p = \rho g z + p_0$ is given by the sum of the ambient and hydrostatic pressure at that depth, up to the cavity wall (where $u_r = \dot{R}$ and $p = p_0$), we obtain

$$\frac{\mathrm{d}}{\mathrm{d}t}(R\dot{R})\int_{R_\infty}^{R}\frac{\mathrm{d}r}{r} + \left[\frac{1}{2}u_r^2\right]_{R_\infty}^{R} = -\left[\frac{p}{\rho}\right]_{R_\infty}^{R},$$

which now directly leads to Equation 3.

When one now solves the equation of motion (Equation 2) for the depth $z(t)$ of the penetrating object as a function of time t, one may invert this expression to obtain the time $t_{\mathrm{pass}}(z)$ at which the object reaches depth z. Subsequently, the 2D Rayleigh-Bésant equation can be solved at any depth z starting from the initial conditions

$$R(t_{\mathrm{pass}}(z); z) = R_0, \qquad \dot{R}(t_{\mathrm{pass}}(z); z) = \beta\dot{z}(t_{\mathrm{pass}}(z)),$$

where R_0 is the radius of the object, and the initial radial expansion velocity of the cavity $\dot{R}$ is assumed to be proportional to the axial velocity $\dot{z}$ of the object at that depth z; i.e., β is a numerical proportionality constant (Duclaux et al. 2007, Bergmann et al. 2009). This finally leads to an approximate description of the time evolution of the cavity profile $R(z, t)$.

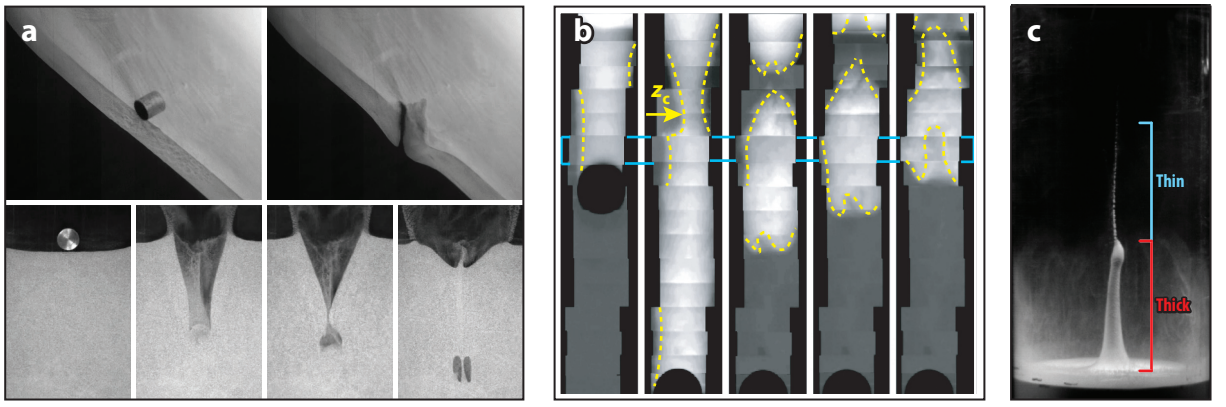

Figure 5

(*a*, *top*) Two snapshots from a tilted top view of a quasi-2D experiment in which a cylinder is dropped onto a confined bed of loose, fine sand. (*Bottom*) Four snapshots showing the cavity formation, collapse, and production of the jet (which now takes the shape of a sheet). Panel *a* adapted with permission from Mikkelsen et al. (2002). Copyright 2002 by the American Institute of Physics. (*b*) Five snapshots from X-ray experiments performed by Royer et al. (2005). One can clearly observe the creation of the cavity, its collapse, and pinch-off and the entrapment of an air bubble (*yellow dashed lines*). In addition, there is a secondary jet-like structure moving upward through the entrapped air bubble. Note that the result has been obtained by stitching together images from repetitions of the experiment. (*c*) Thick-thin structure of the jet. Panels *b* and *c* adapted from Royer et al. (2005) with permission from Macmillan Publishers Ltd.: Nature Physics, copyright 2005.

instantaneous horizontal velocity $\dot{R}$ that follows from the vertical equation of motion for the object (i.e., Equation 2) (Bergmann et al. 2009).

3.1. Granular Jet Formation: Cavity Creation, Collapse, and Pinch-Off

The main question addressed in this section is the extent to which the granular jet is produced from a similar mechanism as in a liquid. After a granular jet had first been observed by Thoroddsen & Shen (2001), who noted the connection to jets in fluids, Lohse et al. (2004a) proposed what they term the cavity collapse mechanism. In fact, these authors presented evidence in the form of quasi-2D experiments in which a cylinder was dropped onto a granular bed confined between two plates (Mikkelsen et al. 2002), such that cavity formation and collapse could be observed from the side (**Figure 5*a***). Indeed, in this quasi-2D experiment, the observations were quite similar to those in a liquid: The impacting cylinder created an, again quasi-2D, cavity, which collapsed because of the hydrostatic (or lithostatic) pressure in the granular bed. At the pinch-off point, two jets were seen to form, one of which moved upward and the other downward, pinching the untrapped air bubble. Note that in this 2D experiment, the jet takes the form of a sheet; therefore, the energy-focusing mechanism present in the 3D axisymmetric system in which all the kinetic energy of the collapsing cavity walls is focused onto a line is absent.

Even more convincing evidence was obtained by Royer et al. (2005), who used a powerful parallel X-ray beam at the Advanced Photon Source (Argonne National Laboratory) to image the full 3D system during impact (**Figure 5*b***) at frame rates up to 5 kHz. Because the beam size limited the field of view to 15×9 mm^2, the authors had to make use of the repeatability of the experiment to image the evolution of the entire cavity by stitching together image sequences obtained at different depths below the surface. The authors also had to use a smaller container and low–atomic number boron carbide particles to obtain sufficient X-ray transmission through the

bed. In doing so, it was, however, verified that the jet production showed no qualitative differences with the larger-scale experiments in sand studied thus far.

In the images, one can clearly observe how the impacting ball creates a cavity and how it collapses and subsequently pinches off, entrapping an air bubble in the process. In addition to a jet moving upward from the pinch-off point, the authors observed a secondary jet-like structure that appears to form from the bottom of the entrapped air bubble. They held this second jet responsible for the formation of what they termed the thick-thin structure of the jet (see **Figure 5*c***) that was observed in certain cases. Royer et al. (2005) argued that the upper, thin part of the jet originated from the central pinch-off point, whereas the lower, thick part stemmed from the bottom of the cavity (i.e., from the lower part of the entrapped air bubble). This point of view was later confirmed by von Kann et al. (2010), who in addition argued that whether this thick-thin structure formed may be connected to the sidewalls, the proximity of which would be able to induce such a double pinch-off event. In fact, Royer et al. (2008) reported multiple pinch-off events entrapping several small air bubbles, but now for small impacting spheres and away from the walls. These repeated pinch-offs were attributed to an underpressure in the entrapped cavity, pulling bed material into it, creating ragged walls that eventually led to multiple entrapped air pockets separated by granular bed material.

Homan et al. (2015) used another X-ray technique to measure the cavity inside, using three industrial X-ray sources complemented with three double arrays of 32 detectors with a sampling frequency of 2.5 kHz. The authors were able to image horizontal cross sections of the (full-size) experiment. Due to reproducibility, they were able to collect experimental runs acquired at different depths below the free surface into a full time evolution of the cavity profile, both qualitatively (**Figure 6*a***) and quantitatively, by combining the transmission data with the geometrical layout of the source-detector arrangement and invoking the expected axisymmetry of the problem (**Figure 6*b***).

In these experiments, the jet formation is clearly observed to arise from the pinch-off point of the collapsing cavity. In fact, even the width of the upgoing jet itself could be measured from the

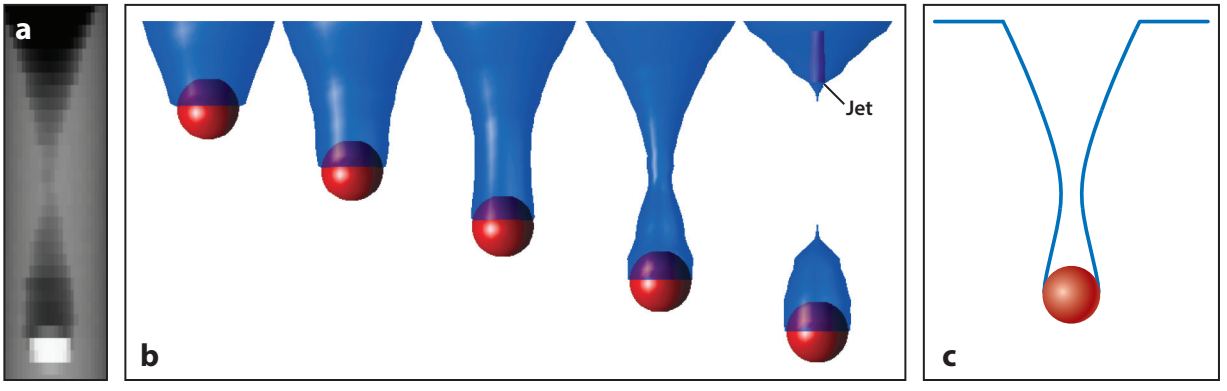

Figure 6

(*a*) Typical intensity plot of the X-ray transmission measured by a detection array. Similar to **Figure 5**, the results have been obtained by combining data from repetitions of the experiment at different heights. (*b*) Reconstruction of the cavity shape from the transmission data at five subsequent moments in time. Note that the upgoing jet is visible in the last snapshot. (*c*) Cavity reconstruction from coupling the drag equation (Equation 2) with the 2D Rayleigh equation (Equation 3) using the initial conditions provided in the sidebar The 2D Rayleigh Equation and the Cavity Profile. Panels *a* and *b* adapted with permission from Homan et al. (2015). Copyright 2015 by Cambridge University Press.

detector signal from the cross sections just above the pinch-off point. Because of the quantitative nature of the data, it was possible to determine the time evolution of the radius of the neck (i.e., the radius at that depth at which the collapsing cavity is the slimmest). From these data, Homan et al. (2015) concluded that within experimental error, the closure of the cavity is at least consistent with the simplified 2D theory of the cavity closure (Equation 3).

Minimal fluidization velocity: minimum upward gas velocity needed to suspend the particles of a granular bed in a gas flow, i.e., to counteract gravity

Figure 6*c* shows the result of a calculation combining the equation of motion (Equation 2), the drag law (Equation 1), and the 2D Rayleigh model (Equation 3), in which the vertical and horizontal motion is coupled using the final equation in the sidebar The 2D Rayleigh Equation and the Cavity Profile. With the measured impact velocity and realistic values for the parameters ($k/m = 3 \times 10^2$ s^{-2}, $\alpha/m = 0$ m^{-1}, $m_A = 0$ kg, $\beta = 0.2$), we obtain realistic cavity shapes; **Figure 6*c*** shows the calculated cavity shape at a time comparable to that at which the fourth snapshot in **Figure 6*b*** was obtained.

3.2. The Role of the Packing Fraction: Compressibility and Cavity Expansion

The issue addressed in this section is the role of the packing fraction in the dynamics of a granular bed. Or, more precisely, how does the packing fraction of the granular bed before impact influence cavity expansion? With the exception of the above-mentioned work of Umbanhowar & Goldman (2010) on the influence of the packing fraction on drag, not much systematic research has been done with respect to its influence on cavity expansion and collapse. However, some general conclusions can be drawn by combining observations from the literature.

To begin, it is clear that the drag on an object is expected to depend strongly on the packing fraction φ, given that, when grains are more densely packed, the force network between them is likely to be stronger and therefore the granular bed less easy to penetrate. This intuitive picture is confirmed by systematic experiments by Umbanhowar & Goldman (2010), who showed that, given a certain impact velocity, the penetration depth of an object decreases with increasing φ. Because one needs a penetration depth of several object diameters to create a cavity, a higher impact velocity is required at higher packing fractions to create a cavity (and a jet).

In fact, after the pioneering experiments of Thoroddsen & Shen (2001), virtually all granular jetting impact experiments have been done with a prefluidization procedure as described by Lohse et al. (2004a): A reproducible initial condition of the bed is obtained by forcing an airflow with a speed above the minimal fluidization velocity through the grains and subsequently slowly turning off the airflow to allow the bed to settle into a very loose packing. As a result, jets have been observed predominantly in granular beds well below the critical packing state, which implies that they can be considered to be compressible. Indeed, X-ray experiments measuring the packing fraction of a granular bed during impact report some compaction of the bed near the cavity walls (Royer et al. 2011, Homan et al. 2015). In addition, the expansion of the cavity in the granular experiments appears to be smaller than in water, which during impact experiments behaves like an incompressible fluid. More quantitatively, Duclaux et al. (2007) reported that the coefficient β in the final equation in the sidebar The 2D Rayleigh Equation and the Cavity Profile, which characterizes the expansion of the cavity, needs to be set to $\beta \approx 0.3$ to fit the data for spheres impacting in water, whereas in a (loosely packed) granular sand bed the required expansion coefficient is smaller, namely $\beta \approx 0.2$.

Finally, the group of Pacheco-Vázquez studied the formation of craters and jets from the implosion of an existing cavity inside the sand created by the means of a balloon (Loranca-Ramos et al. 2015). This work opens the way to studying cavity collapse and jet formation in isolation from impact events.

4. THE INFLUENCE OF INTERSTITIAL AIR

Interstitial air: air that resides within the pores between the grains of a granular medium

When the grain size is small enough, the interstitial air in a granular bed may become important, especially if the air is forced to move in a different manner than the grains of the bed (i.e., when there is a velocity difference ΔV between the grains and air). Let us first provide an estimate of the importance of air drag within the bed. For isolated (spherical) grains, one finds the minimum diameter d below which air becomes important by balancing gravity ($F_g = \rho_g g \pi d^3/6$) and the drag force on the particle in the Stokes' regime ($F_d = 3\pi\mu d V$). Here, $\rho_g \approx 2.5 \times 10^3$ kg/m^3 is the grain density, and $\mu = 1.8 \times 10^{-5}$ Pa·s the dynamic viscosity of air. However, due to the presence of the other grains in a granular packing, the drag force on individual grains is increased by a factor of 40 because the air now needs to flow through the pores in between the drains, which dramatically increases the viscous friction on the particles. If the velocity difference is estimated as the typical velocity of the impacting object, $\Delta V \approx 1$ m/s, then d should be smaller than ≈0.7 mm to observe an effect of the air.

However, because it is expected that the grains and air set in motion by the impacting object will move at approximately the same speed, the velocity scale taken in the above calculation appears to be greatly exaggerated. The velocity difference between the two phases may be as small as a few millimeters per second, especially when the object has completely penetrated into the sand and the grains that would somewhat suffer the effect from such a flow rate should be smaller than 50 μm in diameter. The anticipated influence of the interstitial air was therefore expected to be small, if not marginal. The reverse, however, turned out to be true.

4.1. Jet Formation at Reduced Ambient Pressure

Royer et al. (2005) were the first to systematically vary the ambient air pressure P_0 during impact experiments. The whole setup was made such that—after the prefluidization procedure described in Section 3—it could be evacuated slowly without disturbing the very loose packing of the granular bed. They observed a profound influence on the jet height: Reducing the air pressure from atmospheric values (101 kPa) to a reduced value $P_0 = 2.7$ kPa caused a reduction in the jet height of over 70% (**Figure 7*a***). Not only was the height of the jet strongly affected, but its thickness was as well, which makes the whole jet phenomenon appear feeble and weak at low P_0 in comparison to its atmospheric pressure counterpart. The big question, however, was what caused this large reduction in jet size. Early hypotheses included an effect of the pressurization of the entrapped air bubble, which would support the formation of the jet at higher pressures and thus aid in the production of a thicker, stronger jet at high ambient pressures.

Measuring the trajectory of the object inside the granular bed—as was undertaken simultaneously and independently by Royer et al. (2007) and Caballero et al. (2007)—provided a large part of the answer. For the same impact velocity, the impacting object would penetrate much deeper when the ambient pressure was closer to the atmospheric pressure (**Figure 7*b***). In fact, Caballero et al. (2007) measured the jet height and penetration depth simultaneously (**Figure 7*c***) and found that the penetration depth decreases continuously with decreasing ambient pressure. However, if one monitors the trajectory of the impacting sphere up to the moment in time at which the cavity closes (which incidentally appears to be largely independent of P_0), there are no significant changes down to a pressure of 400 mbar. Since this would leave the location of the pinch-off point unaltered, the authors concluded that this explains why the jet height remains largely unchanged when P_0 is lowered from its atmospheric value to 400 mbar. However, when P_0 was lowered even further, they observed significant changes in the trajectory before the closure time, which must cause the cavity to close at a shallower point, closer to the free surface of the granular bed. Because the hydrostatic pressure that drives the collapse is smaller

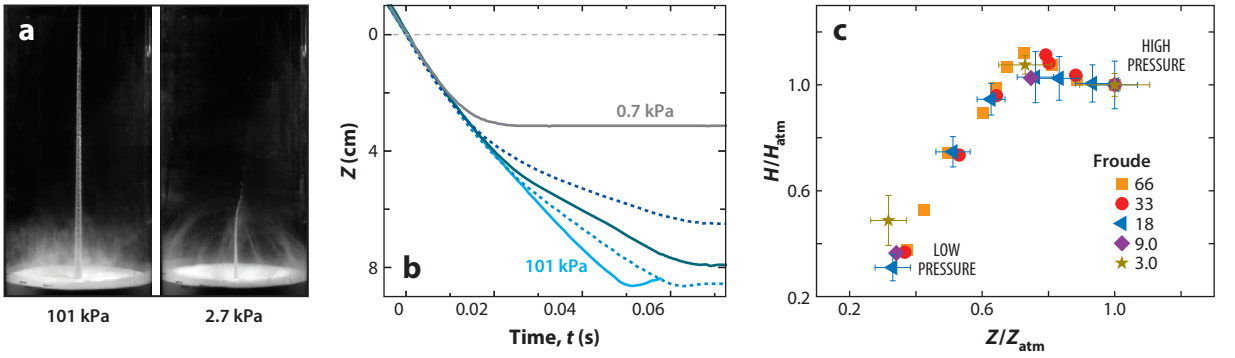

Figure 7

(*a*) Jets resulting from impact at the same speed but at different ambient pressures. The jet at reduced ambient pressure is observed to be much weaker (Royer et al. 2005, 2008). (*b*) Trajectories $z(t)$ obtained from high-speed X-ray imaging of a sphere penetrating a loose granular bed (Royer et al. 2007). When the pressure is reduced, the sphere penetrates less deep. (*c*) Maximum jet height H versus penetration depth Z resulting from impact of a sphere at reduced ambient pressures, for different values of the impact velocity V, reflected in the Froude number $\mathrm{Fr} = V^2/(gD)$, with D the sphere diameter. Both H and Z are normalized by their respective values H_{atm} and Z_{atm} obtained under atmospheric conditions. When the ambient pressure decreases, the penetration depth decreases as well, whereas the jet height first remains approximately constant up to $P_0 \approx 400$ mbar, below which it also starts to decrease. Panels *a*, *b*, and *c* adapted with permission from Royer et al. (2008), Royer et al. (2007), and Caballero et al. (2007), respectively. Copyright 2007 and 2008 by the American Physical Society.

at this shallower depth, they argued that this will lead to a smaller jet height. In **Figure 7*c***, the transition point located at $Z \approx 0.75 Z_{\mathrm{atm}}$ that separates a constant jet height H region from a region where H appears to linearly depend on Z corresponds to an ambient pressure value of $P_0 = 400$ mbar.

The conclusion was that the jet formation phenomenon depends on ambient pressure because the drag an object experiences in a loosely packed granular bed consisting of small grains decreases with P_0. In fact, the coefficient k introduced in Equation 1 has been measured as a function of P_0 by Caballero et al. (2007) and was found to roughly increase as $P_0^{-1/2}$ for decreasing ambient pressure. The remaining question, namely why and how the drag depends on P_0, is addressed in the next subsection.

4.2. Direct Measurement of the Drag Force on an Impacting Object

In what way can air present in the pores between the grains in a granular bed influence the dynamics of the bed? One of the most striking examples found in the literature is the so-called blown air effect discussed by Clément et al. (2011), who showed that it is easier to push a glass upside down into a granular bed than an open cylinder of the same dimensions (**Figure 8*a***). This is a result of the airflow set up inside the sand along the rim of the glass because air must escape from the glass when it is pushed in: This airflow dilates the sand and thus allows the glass to move in with considerably less friction than there would be without the air.

Dilate: to expand sand such that its packing fraction is at or below the critical packing state

Other examples of how air affects the dynamics of a dense granular system include the production of so-called Faraday heaps on a vertically vibrated layer of millimeter-sized grains (Pak et al. 1995; van Gerner et al. 2007, 2009; Pastenes et al. 2014; van Gerner et al. 2015), the role of air in the Brazil nut effect (Möbius et al. 2001, 2005), and the reversal of the Chladni patterns observed on a vibrating plate (van Gerner et al. 2011).

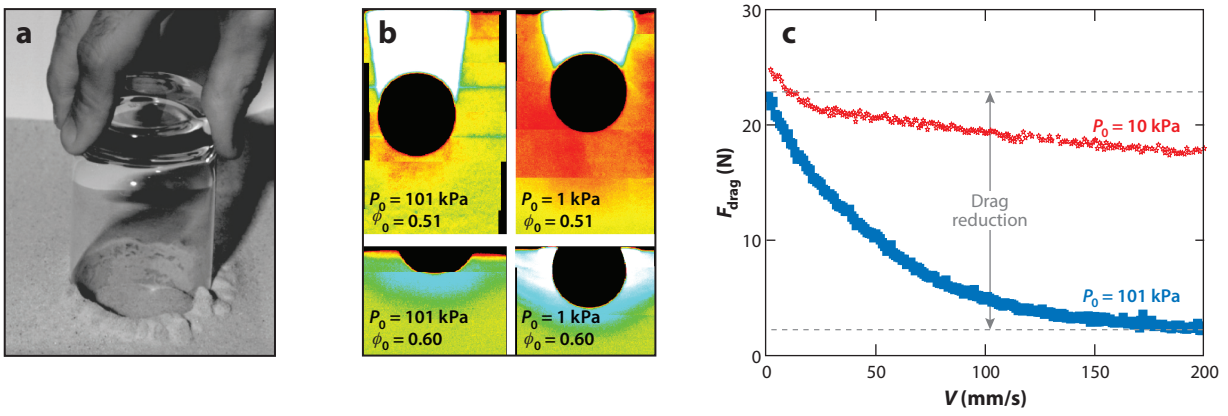

Figure 8

(*a*) The blown air effect explains why it is relatively easy to push a reversed glass into a granular bed (Clément et al. 2011). (*b*) Four snapshots, all taken at $t = 10$ ms after the impact of a sphere dropped from the same height ($h = 35$ cm), using X-ray imaging, showing the changes in the packing fraction with respect to the pre-impact average (*yellow*). An increase in the packing fraction (compaction) is denoted by red, and a decrease (expansion or dilation) by light colors. Clearly, compaction and dilation are less pronounced at atmospheric pressure than at reduced ambient pressure (Royer et al. 2011). (*c*) Drag force F_{drag} measured at a depth of 10 cm below the surface for a sphere pushed with a constant velocity V into a loose granular bed by a penetrometer. At atmospheric pressures, F_{drag} decreases from a quasi-static value of 23 N to 2 N at the maximum velocity $V = 0.2$ m/s. At a reduced pressure ($P_0 = 100$ mbar), this drag reduction is much less pronounced, showing that the drag reduction is the result of air trapped in the pores between the grains (Homan & van der Meer 2016). Panel *a* reprinted with permission from Clément et al. (2011). Copyright 2011 by the American Physical Society. Panel *b* adapted with permission from Royer et al. (2011). Copyright 2011 by EDP Sciences.

From the above examples, it is clear that air can locally strongly affect the dynamics of the sand. But to know in what way this happens, we need to look at where the air is located in the granular impact experiments discussed here. An important step was taken by Royer et al. (2011), who compared the effect of the impact of a steel sphere on the packing fraction of a granular bed for a loose bed ($\varphi = 0.51$) and a compacted bed ($\varphi = 0.60$), both at atmospheric ($P_0 = 101$ kPa) and at reduced ($P_0 = 1$ kPa) ambient pressures. They observed that at reduced ambient pressure, there was a significant compaction of the loosely packed bed just below the impactor, whereas in the dense bed there was significant dilation (**Figure 8*b***), as would be expected to allow for the motion of the grains that is necessary for the sphere to penetrate into the sand. At atmospheric pressures, however, compaction and dilatation were much less pronounced, if at all present. Royer et al. (2011, p. 4) then drew the important conclusion that "during sudden impact, the primary role of the interstitial air in a fine-grained granular bed is to oppose changes in the bed packing density."

Now, how does air get trapped inside the granular bed? Using Darcy's law and mass conservation, one can derive the following equation for the excess gas pressure $\Delta P = P - P_0$ inside the granular medium (Gutman & Davidson 1975, Pak et al. 1995, McNamara et al. 2000, Möbius et al. 2005, Anghel et al. 2006, Royer et al. 2008, Homan et al. 2014):

$$\frac{\partial \Delta P}{\partial t} = D\nabla^2(\Delta P) + \frac{P_0}{1-\varphi}\frac{\partial \varphi}{\partial t}, \tag{4}$$

as shown in the sidebar Porous Media Equation in a Granular Medium. This is a diffusion equation with a source term that depends on the rate of change of the packing fraction inside the granular bed. Royer et al. (2011) used this equation to explain their observations. They argued that, because the source term is proportional to P_0, at high ambient pressures the magnitude of the pressure

POROUS MEDIA EQUATION IN A GRANULAR MEDIUM

Darcy's law for the volume flux $\mathbf{q}$ of air into an infinitesimally small volume δV of a granular porous medium (Darcy 1856, Carman 1956) states that

$$\mathbf{q} = -\frac{\kappa}{\mu}\nabla P,$$

where κ is the permeability of the porous medium and μ the dynamic viscosity of air. With this volume flux, mass conservation for the air present in the volume can be expressed as

$$\frac{\partial(\rho(1-\varphi))}{\partial t}\,\delta V = -\nabla\cdot(\rho\mathbf{q})\,\delta V,$$

where φ is the packing fraction of the granular medium, such that $(1-\varphi)$ is the fraction of the volume that is occupied by air. In the above equation, ρ is the air density, which with the ideal gas law ($P = \rho RT$) can be expressed in terms of the pressure P. Here, R is the specific gas constant of air and T the temperature. For most conditions encountered during impact experiments, T can be assumed to be constant owing to the good thermal contact with the grains and their comparatively large heat capacity. The two equations above can then be directly combined into the porous media equation

$$\frac{\partial(P(1-\varphi))}{\partial t} = \frac{\kappa}{\mu}\nabla^2(P^2),$$

with ∇^2 the Laplacian. Writing $P = P_0 + \Delta P$ and linearizing in ΔP, we obtain

$$\frac{\partial \Delta P}{\partial t} = D\,\nabla^2(\Delta P) + \frac{P_0}{1-\varphi}\frac{\partial \varphi}{\partial t},$$

which is a diffusion equation with diffusivity D given by $D = 2\kappa P_0/(\mu(1-\varphi))$ and containing a source term that is proportional to the ambient pressure P_0 and the time rate of change of the packing fraction φ of the granular medium. This is Equation 4 provided in the main text.

built up in front of the sphere would also be large; therefore, the grains would resist compaction or dilation.

Homan et al. (2014) applied Equation 4 to a very loose granular bed of the type used in the impact experiments, which was collapsed by supplying an external tap to the container of varying strength and at different ambient pressures. They found that, whereas the bed collapsed on a timescale of milliseconds, air was trapped inside the bed and diffused out on the much longer timescale of (in some cases) seconds, as dictated by the diffusion coefficient D. Moreover, the relaxation of the pressure turned out to be quantitatively well described by Equation 4.

The behavior of the drag at different penetration velocities V and ambient pressures P_0 was directly measured by Homan & van der Meer (2016), who used a linear motor to push a sphere inside the sand and at the same time measured the drag force that the sand exerts on it. The main result of this modified penetrometer experiment (cf. Stone et al. 2004 and Albert et al. 2001 for the original penetrometer experiment) is plotted in **Figure 8*c***: For very small penetration velocities ($V = 1$ mm/s), they observed a quasi-static limit in which the drag becomes independent of the ambient pressure. For atmospheric pressure, the drag decreases dramatically with the penetration velocity until it reaches a plateau of less than 20% of the quasi-static value. At a reduced ambient pressure of 100 mbar, however, the drag decreases much less, thereby confirming that the drag reduction is an air effect. Using Equation 4, Homan & van der Meer (2016) constructed a model that quantitatively explains their observations.

5. CONCLUDING REMARKS

This review is concluded with a short summary of its contents, for which the reader is referred to the Summary Points section below. In addition, a number of future issues can be identified that need to be addressed to make progress in our understanding of the impact of objects onto granular beds. Of course, this view is biased by the current research interests of the author and necessarily limited by his scientific horizon, and therefore does not pretend to be in any way complete.

Recent developments have been made in many areas that are, sometimes intimately, connected to the subject of this study. Although a full description would go beyond the scope of this review, here I mention the most significant ones.

There are several papers that deal with the splash formed upon impact (Deboeuf et al. 2009, Marston et al. 2012a, Caballero-Robledo et al. 2012) and with impact cratering from a physics perspective (Amato & Williams 1998, Zheng et al. 2004, Boudet et al. 2006, Nishida et al. 2010).

Also, the air in a granular substrate can be (partly) replaced by water, which is quite relevant from the perspective of applications and creates wet granular packings that are usually stiffer than the dry granular beds discussed in this article (Marston et al. 2012b, Tiwari et al. 2014, Brzinski et al. 2015). On the other end of the spectrum, one can create very loose, mechanically unstable granular beds by fluidizing during impact, such that there is still gas flow through the bed while the object penetrates (Marston et al. 2008, Brzinski & Durian 2010, Brzinski et al. 2013). This is connected to gas-fluidized beds, a well-studied class of systems that is widely applied in many chemical processes (van der Hoef et al. 2008).

Finally, a number of scientists recently became interested in the impact of raindrops, i.e., what happens when a water droplet impacts onto a granular substrate (Katsuragi 2010, 2011; Delon et al. 2011; Marston et al. 2010, 2012c; Emady et al. 2012; Nefzaoui & Skurtys 2012; Long et al. 2014; R. Zhao et al. 2015; S. Zhao et al. 2015). Now not only does the substrate deform during impact, but also does the impacting droplet. When the grains are wetted by the droplet liquid, the impactor and substrate may mix during impact, leaving substrates that may resemble a pancake, donut, or truffle, depending on the degree of mixing.

Partly inspired by these newer lines of research and partly by the unresolved issues discussed in the previous sections, this leads to a number of points that could well be addressed in future work. These points are listed in the Future Issues section below.

SUMMARY POINTS

1. The impact of an object on a granular bed bears many similarities with that on a liquid substrate, especially when the bed is loosely packed and consists of small grains.
2. Although a granular bed behaves similarly to a liquid as soon as it is fluidized by the impact, the fact that in the end it turns into a solid again leads to remarkable differences, such as that an impact crater usually forms at the free surface and that the object gets stuck somewhere in the bulk of the bed. This is different from a liquid where the object continues to move.
3. The creation of a cavity, its collapse, and the formation of the jet all proceed along similar lines as with the impact on a liquid. Given a certain penetration depth, these stages appear to be hardly affected by ambient pressure.
4. Surprisingly, the drag the object experiences in a loose granular bed is strongly affected by ambient air pressure. Interstitial air causes the drag to decrease significantly from its quasi-static value.

FUTURE ISSUES

1. Although some knowledge has been obtained about the influence of ambient air pressure on drag, it is crucial to investigate and understand the role played by the packing fraction for a full understanding of the phenomenon.
2. It will be worthwhile to study the behavior of a granular bed while tuning it from a static, solid-like substrate to a liquid using fluidization.
3. It is essential to disentangle the different mechanisms at play for a full understanding of droplet impacts on sand: droplet deformation, substrate deformation, and droplet-substrate mixing.

DISCLOSURE STATEMENT

The author is not aware of any biases that might be perceived as affecting the objectivity of this review.

ACKNOWLEDGMENTS

I am very grateful to all coworkers, colleagues, and collaborators for their contributions to our understanding of this wonderfully rich system, for the many stimulating discussions I enjoyed with them, and for carefully reading the manuscript and/or for providing valuable comments. I also gratefully acknowledge FOM and the Netherlands Organisation for Scientific Research (NWO) for financial support over the years. This work is part of the VIDI project 68047512, which is financed by NWO.

LITERATURE CITED

Aguilar J, Goldman DI. 2016. Robophysical study of jumping dynamics on granular media. *Nat. Phys.* 12:278–83

Albert I, Sample JG, Morss AJ, Rajagopalan S, Barabási AL, Schiffer P. 2001. Granular drag on a discrete object: shape effects on jamming. *Phys. Rev. E* 64:061303

Allen WA, Mayfield EB, Morrison HL. 1957. Dynamics of a projectile penetrating sand. *J. Appl. Phys.* 28:370–76

Altshuler E, Torres H, González Pita A, Sánchez Colina G, Pérez Penichet C, et al. 2014. Settling into dry granular media in different gravities. *Geophys. Res. Lett.* 41:3032–37

Amato JC, Williams RE. 1998. Crater formation in the laboratory: an introductory experiment in error analysis. *Am. J. Phys.* 66:141–43

Ambroso MA, Kamien RD, Durian DJ. 2005a. Dynamics of shallow impact cratering. *Phys. Rev. E* 72:041305

Ambroso MA, Santore CR, Abate AR, Durian DJ. 2005b. Penetration depth for shallow impact cratering. *Phys. Rev. E* 71:051305

Anghel DV, Strauss M, McNamara S, Flekkøy EG, Måløy KJ. 2006. Erratum: Grains and gas flow: molecular dynamics with hydrodynamic interactions. *Phys. Rev. E* 74:029906

Aranson IS, Tsimring LS. 2006. Patterns and collective behavior in granular media: theoretical concepts. *Rev. Mod. Phys.* 78:641–92

Backman ME, Goldsmith W. 1978. The mechanics of penetration of projectiles into targets. *Int. J. Eng. Sci.* 16:1–99

Bartali R, Rodriguez-Liñán GM, Nahmad-Molinari Y, Sarocchi D, Ruiz-Suárez JC. 2013. Role of the granular nature of meteoritic projectiles in impact crater morphogenesis. arXiv:1302.0259 [astro-ph.EP]

Ben-Dor G, Dubinsky A, Elperin T. 2009. Modeling of penetration by rigid impactors. *Mech. Res. Commun.* 36:625–29
Bergmann R, Stijnman M, Sandtke M, van der Meer D, Prosperetti A, Lohse D. 2006. Giant bubble collapse. *Phys. Rev. Lett.* 96:154505
Bergmann R, van der Meer D, Gekle S, van der Bos A, Lohse D. 2009. Controlled impact of a disk on a water surface: cavity dynamics. *J. Fluid Mech.* 633:381–409
Boguslavskii Y, Drabkin S, Juran I, Salman A. 1996a. Theory and practice of projectile's penetration in soils. *J. Geotechnol. Eng.* 122:806–10
Boguslavskii Y, Drabkin S, Salman A. 1996b. Analysis of vertical projectile penetration in granular soils. *J. Phys. D* 29:905–16
Boudet JF, Amarouchene Y, Kellay H. 2006. Dynamics of impact cratering in shallow sand layers. *Phys. Rev. Lett.* 96:158001
Brzinski TA III, Durian DJ. 2010. Characterization of the drag force in an air-moderated granular bed. *Soft Matter* 6:3038–43
Brzinski TA III, Mayor P, Durian DJ. 2013. Depth-dependent resistance of granular media to vertical penetration. *Phys. Rev. Lett.* 111:168002
Brzinski TA III, Schug J, Mao K, Durian DJ. 2015. Penetration depth scaling for impact into wet granular packings. *Phys. Rev. E* 91:022202
Caballero G, Bergmann R, van der Meer D, Prosperetti A, Lohse D. 2007. Role of air in granular jet formation. *Phys. Rev. Lett.* 99:018001
Caballero-Robledo GA, Kelly KP, Homan TAM, Weijs JH, van der Meer D, Lohse D. 2012. Suction of splash after impact on dry quick sand. *Granul. Matter* 14:179–84
Carman PC. 1956. *Flow of Gases Through Porous Media*. London: Butterworths Sci.
Ciamarra MP, Lara AH, Lee AT, Goldman DI, Vishik I, Swinney HL. 2004. Dynamics of drag and force distributions for projectile impact in a granular medium. *Phys. Rev. Lett.* 92:194301
Clark AH, Behringer RP. 2013. Granular impact model as an energy-depth relation. *Eur. Phys. Lett.* 101:64001
Clark AH, Kondic L, Behringer RP. 2012. Particle scale dynamics in granular impact. *Phys. Rev. Lett.* 109:238302
Clark AH, Petersen AJ, Behringer RP. 2014. Collisional model for granular impact dynamics. *Phys. Rev. E* 89:012201
Clément R, Courrech du Pont S, Ould-Hamouda M, Duveau D, Douady S. 2011. Penetration and blown air effect in granular media. *Phys. Rev. Lett.* 106:098001
Daniels KE, Coppock JE, Behringer RP. 2004. Dynamics of meteor impacts. *Chaos* 14:S4
Darcy HPG. 1856. *Les fontaines publiques de la ville de Dijon*. Paris: Victor Dalmont
de Bruyn JR, Walsh AM. 2004. Penetration of spheres into loose granular media. *Can. J. Phys.* 82:439–46
de Gennes PG. 1999. Granular matter: a tentative view. *Rev. Mod. Phys.* 71:S374
Deboeuf S, Gondret P, Rabaud M. 2009. Dynamics of grain ejection by sphere impact on a granular bed. *Phys. Rev. E* 79:041306
Delon G, Terwagne D, Dorbolo S, Vandewalle N, Caps H. 2011. Impact of liquid droplets on granular media. *Phys. Rev. E* 84:046320
Duclaux V, Caillé F, Duez C, Ybert C, Bocquet L, Clanet C. 2007. Dynamics of transient cavities. *J. Fluid Mech.* 591:1–19
Dwivedi SK, Teeter RD, Felice CW, Gupta YM. 2008. Two dimensional mesoscale simulations of projectile instability during penetration in dry sand. *J. Appl. Phys.* 104:083502
Emady HN, Kayrak-Talay D, Schwerin WC, Litster JD. 2012. A regime map for granule formation by drop impact on powder beds. *Powder Technol.* 212:69–79
Gekle S, Gordillo JM, van der Meer D, Lohse D. 2009. High-speed jet formation after solid object impact. *Phys. Rev. Lett.* 102:034502
Goldman DI, Umbanhowar P. 2008. Scaling and dynamics of sphere and disk impact into granular media. *Phys. Rev. E* 77:021308
González Gutiérrez J, Carrillo Estrada JL, Ruiz Suárez JC. 2014. Penetration of granular projectiles into a water target. *Sci. Rep.* 4:6762

Gutman RG, Davidson JF. 1975. Darcy's law for oscillatory flow. *Chem. Eng. Sci.* 30:89–95
Hinch J. 2014. Particles impacting on a granular bed. *J. Eng. Math.* 84:41–48
Holsapple KA. 1993. The scaling of impact processes in planetary science. *Annu. Rev. Earth Planet. Sci.* 21:333–73
Holsapple KA, Giblin I, Housen K, Nakamura A, Ryan E. 2002. Asteroid impacts: laboratory experiments and scaling laws. In *Asteroid III*, ed. W Bottke, A Cellino, P Paolicchi, RP Binzel, pp. 443–62. Tucson: Univ. Ariz. Press
Homan TAM, Gjaltema C, van der Meer D. 2014. Collapsing granular beds: the role of interstitial air. *Phys. Rev. E* 89:052204
Homan TAM, Mudde R, Lohse D, van der Meer D. 2015. High-speed X-ray imaging of a ball impacting on loose sand. *J. Fluid Mech.* 777:690–706
Homan TAM, van der Meer D. 2016. Giant drag reduction due to interstitial air in sand. arXiv:1607.07774 [cond-mat.soft]
Hou M, Peng Z, Liu R, Lu K, Chan CK. 2005a. Dynamics of a projectile penetrating in granular systems. *Phys. Rev. E* 72:062301
Hou M, Peng Z, Liu R, Wu Y, Tian Y, et al. 2005b. Projectile impact and penetration in loose granular bed. *Sci. Technol. Adv. Mater.* 6:855–59
Jaeger HM, Nagel SR, Behringer RP. 1996a. Granular solids, liquids, and gases. *Rev. Mod. Phys.* 68:1259–73
Jaeger HM, Nagel SR, Behringer RP. 1996b. The physics of granular materials. *Phys. Today* 49:32–39
Janssen HA. 1895. Versuche uber getreidedruck in silozellen. *Dtsch. Ing.* 39:1045
Joubaud S, Homan TAM, Gasteuil Y, Lohse D, van der Meer D. 2014. Forces encountered by a sphere during impact into sand. *Phys. Rev. E* 90:060201
Kadanoff LP. 1999. Built upon sand: theoretical ideas inspired by granular flows. *Rev. Mod. Phys.* 71:435–44
Katsuragi H. 2010. Morphology scaling of drop impact onto a granular layer. *Phys. Rev. Lett.* 104:218001
Katsuragi H. 2011. Length and time scales of a liquid drop impact and penetration into a granular layer. *J. Fluid Mech.* 675:552–73
Katsuragi H. 2016. *Physics of Soft Impact and Cratering*. New York: Springer
Katsuragi H, Durian DJ. 2007. Unified force law for granular impact cratering. *Nat. Phys.* 3:420–23
Katsuragi H, Durian DJ. 2013. Drag force scaling for penetration into granular media. *Phys. Rev. E* 87:052208
Kondic L, Fang X, Losert W, O'Hern CS, Behringer RP. 2012. Microstructure evolution during impact on granular matter. *Phys. Rev. E* 85:011305
Lohse D, Bergmann R, Mikkelsen R, Zeilstra C, van der Meer D, et al. 2004a. Impact on soft sand: void collapse and jet formation. *Phys. Rev. Lett.* 93:198003
Lohse D, Rauhé R, Bergmann R, van der Meer D. 2004b. Creating a dry variety of quicksand. *Nature* 432:689–90
Long EJ, Hargrave GK, Cooper JR, Kitchener BGB, Parsons AJ, et al. 2014. Experimental investigation into the impact of a liquid droplet onto a granular bed using three-dimensional, time-resolved, particle tracking. *Phys. Rev. E* 89:032201
Loranca-Ramos FE, Carrillo-Estrada JL, Pacheco-Vázquez F. 2015. Craters and granular jets generated by underground cavity collapse. *Phys. Rev. Lett.* 115:028001
Marston JO, Li EQ, Thoroddsen ST. 2012a. Evolution of fluid-like granular ejecta generated by sphere impact. *J. Fluid Mech.* 704:5–36
Marston JO, Seville JPK, Cheun YV, Ingram A, Decent SP, Simmons MJH. 2008. Effect of packing fraction on granular jetting from solid sphere entry into aerated and fluidized beds. *Phys. Fluids* 20:023301
Marston JO, Thoroddsen S, Ng W, Tan R. 2010. Experimental study of liquid drop impact onto a powder surface. *Powder Technol.* 203:223–36
Marston JO, Vakarelski IU, Thoroddsen ST. 2012b. Sphere impact and penetration into wet sand. *Phys. Rev. E* 86:020301
Marston JO, Zhu Y, Vakarelski IU, Thoroddsen ST. 2012c. Drop spreading and penetration into pre-wetted powders. *Powder Technol.* 228:424–28
McNamara S, Flekkøy EG, Måløy KJ. 2000. Grains and gas flow: molecular dynamics with hydrodynamic interactions. *Phys. Rev. E* 61:4054–59

Melosh HJ. 1989. *Impact Cratering: A Geological Process*. Oxford, UK: Oxford Univ. Press
Melosh HJ, Ivanov BA. 1999. Impact crater collapse. *Annu. Rev. Earth Planet. Sci.* 27:385–415
Mikkelsen R, Versluis M, Koene E, Bruggert GW, van der Meer D, et al. 2002. Granular eruptions: void collapse and jet formation. *Phys. Fluids* 14:S14
Möbius ME, Cheng X, Eshuis P, Karczmar GS, Nagel SR, Jaeger HM. 2005. Effect of air on granular size separation in a vibrated granular bed. *Phys. Rev. E* 72:011304
Möbius ME, Lauderdale BE, Nagel SR, Jaeger HM. 2001. Brazil-nut effect: size separation of granular particles. *Nature* 414:270
Nefzaoui E, Skurtys O. 2012. Impact of a liquid drop on a granular medium: inertia, viscosity and surface tension effects on the drop deformation. *Exp. Therm. Fluid Sci.* 41:43–50
Nelson EL, Katsuragi H, Mayor P, Durian DJ. 2008. Projectile interactions in granular impact cratering. *Phys. Rev. Lett.* 101:068001
Newhall KA, Durian DJ. 2003. Projectile-shape dependence of impact craters in loose granular media. *Phys. Rev. E* 68:060301
Nishida M, Okumura M, Tanaka K. 2010. Effects of density ratio and diameter ratio on critical incident angles of projectiles impacting granular media. *Granul. Matter* 12:337–44
Nordstrom K, Lim E, Harrington M, Losert W. 2014. Granular dynamics during impact. *Phys. Rev. Lett.* 112:228002
Pacheco-Vázquez F, Caballero-Robledo GA, Solano-Altamirano JM, Altshuler E, Batista-Leyva AJ, Ruiz-Suárez JC. 2011. Infinite penetration of a projectile into a granular medium. *Phys. Rev. Lett.* 106:218001
Pacheco-Vázquez F, Ruiz-Suárez JC. 2009. Sliding through a superlight granular medium. *Phys. Rev. E* 80:060301
Pacheco-Vázquez F, Ruiz-Suárez JC. 2010. Cooperative dynamics in the penetration of a group of intruders in a granular medium. *Nat. Commun.* 1:123
Pacheco-Vázquez F, Ruiz-Suárez JC. 2011. Impact craters in granular media: grains against grains. *Phys. Rev. Lett.* 107:218001
Pak HK, van Doorn E, Behringer RP. 1995. Effects of ambient gases on granular materials under vertical vibration. *Phys. Rev. Lett.* 74:4643–46
Pastenes JC, Géminard JC, Melo F. 2014. Interstitial gas effect on vibrated granular columns. *Phys. Rev. E* 89:062205
Pierazzo E, Collins G. 2004. A brief introduction to hydrocode modeling of impact cratering. In *Cratering in Marine Environments and on Ice*, ed. H Dypvik, MJ Burchell, P Claeys, pp. 323–40. New York: Springer
Poncelet JV. 1829. *Cours de mécanique industrielle*. Metz
Royer JR, Conyers B, Corwin EI, Eng PJ, Jaeger HM. 2011. The role of interstitial gas in determining the impact response of granular beds. *Europhys. Lett.* 93:28008
Royer JR, Corwin EI, Conyers B, Flior A, Rivers ML, et al. 2008. Birth and growth of a granular jet. *Phys. Rev. E* 78:011305
Royer JR, Corwin EI, Flior A, Cordero ML, Rivers ML, et al. 2005. Formation of granular jets observed by high-speed X-ray radiography. *Nat. Phys.* 1:164–67
Royer JR, Corwin EI, Rivers ML, Eng PJ, Jaeger HM. 2007. Gas-mediated impact dynamics in fine-grained granular materials. *Phys. Rev. Lett.* 99:038003
Ruiz Suárez JC. 2013. Penetration of projectiles into granular targets. *Rep. Prog. Phys.* 76:066601
Schofield AN, Wroth CP. 1968. *Critical State Soil Mechanics*. London: McGraw-Hill
Schröter M, Nägle S, Radin C, Swinney HL. 2007. Phase transition in a static granular system. *Eur. Phys. Lett.* 78:44004
Seguin A, Bertho Y, Gondret P, Crassous J. 2009. Sphere penetration by impact in a granular medium: a collisional process. *Eur. Phys. Lett.* 88:44002
Solano-Altamirano JM, Caballero-Robledo GA, Pacheco-Vázquez F, Kamphorst V, Ruiz-Suárez JC. 2013. Flow-mediated coupling on projectiles falling in a superlight granular medium. *Phys. Rev. E* 88:032206
Sperl M. 2006. Experiments on corn pressure in silo cells: translation and comment of Janssen's paper from 1895. *Granul. Matter* 8:59–65
Stone MB, Barry R, Bernstein DP, Pelc MD, Tsui YK, Schiffer P. 2004. Local jamming via penetration of a granular medium. *Phys. Rev. E* 70:041301

Thoroddsen ST, Etoh TG, Takehara K. 2008. High-speed imaging of drops and bubbles. *Annu. Rev. Fluid Mech.* 40:257–85

Thoroddsen ST, Shen AQ. 2001. Granular jets. *Phys. Fluids* 13:4–6

Tiwari M, Krishna Mohan TR, Sen S. 2014. Penetration depth scaling for impact into wet granular packings. *Phys. Rev. E* 90:062202

Tsimring LS, Volfson D. 2005. Modeling of impact cratering in granular media. *Powders Grains* 2:1215–23

Uehara JS, Ambroso MA, Ojha RP, Durian DJ. 2003. Low-speed impact craters in loose granular media. *Phys. Rev. Lett.* 90:194301. Erratum. 2003. *Phys. Rev. Lett.* 91:149902

Umbanhowar P, Goldman DI. 2010. Granular impact and the critical packing state. *Phys. Rev. E* 82:010301

van der Hoef MA, van Sint Annaland M, Deen NG, Kuipers JAM. 2008. Numerical simulation of dense gas-solid fluidized beds: a multiscale modeling strategy. *Annu. Rev. Fluid Mech.* 40:47–70

van Gerner HJ, Caballero-Robledo GA, van der Meer D, van der Weele K, van der Hoef MA. 2009. Coarsening of Faraday heaps: experiment, simulation, and theory. *Phys. Rev. Lett.* 103:028001

van Gerner HJ, van der Hoef MA, van der Meer D, van der Weele K. 2007. The interplay of air and sand: Faraday heaping unravelled. *Phys. Rev. E* 76:051305

van Gerner HJ, van der Weele K, van der Hoef MA, van der Meer D. 2011. Air-induced inverse Chladni patterns. *J. Fluid Mech.* 689:203–20

van Gerner HJ, van der Weele K, van der Meer D, van der Hoef MA. 2015. Scaling behavior of coarsening Faraday heaps. *Phys. Rev. E* 92:042203

Versluis M. 2013. High-speed imaging in fluids. *Exp. Fluids* 54:1458

Volfson D, Tsimring LS, Aranson IS. 2003. Partially fluidized shear granular flows: continuum theory and molecular dynamics simulations. *Phys. Rev. E* 68:021301

von Kann S, Joubaud S, Caballero-Robledo GA, Lohse D, van der Meer D. 2010. Effect of finite container size on granular jet formation. *Phys. Rev. E* 81:041306

Walsh AM, Holloway KE, Habdas P, de Bruyn JR. 2003. Morphology and scaling of impact craters in granular media. *Phys. Rev. Lett.* 91:104301

Worthington AM. 1908. *A Study of Splashes*. London: Longmans, Green & Co.

Xu Y, Padding JT, Kuipers JAM. 2014. Numerical investigation of the vertical plunging force of a spherical intruder into a prefluidized granular bed. *Phys. Rev. E* 90:062203

Xu Y, Padding JT, van der Hoef MA, Kuipers JAM. 2013. Detailed numerical simulation of an intruder impacting on a granular bed using a hybrid discrete particle and immersed boundary (DP-IB) method. *Chem. Eng. Sci.* 104:201–7

Zhao R, Zhang Q, Tjugito H, Cheng X. 2015. Drop spreading and penetration into pre-wetted powders. *PNAS* 112:342–47

Zhao SC, de Jong R, van der Meer D. 2015. Raindrop impact on sand: a dynamic explanation of crater morphologies. *Soft Matter* 11:6562–68

Zheng XJ, Wang ZT, Qiu ZG. 2004. Impact craters in loose granular media. *Eur. Phys. J.* 13:321–24

Annual Review of Fluid Mechanics
Volume 49, 2017

Contents

Indexes

Errata

An online log of corrections to *Annual Review of Fluid Mechanics* articles may be found at http://www.annualreviews.org/errata/fluid